

Exchange interaction and magnetic domain formation in periodically inhomogeneous magnetic media

S. Blomeier* and B. Hillebrands

Fachbereich Physik und Forschungsschwerpunkt MINAS, Technische Universität Kaiserslautern, 67663 Kaiserslautern, Germany

B. Reuscher, A. Brodyanski, and M. Kopnarski

Institut für Oberflächen- und Schichtanalytik, Technische Universität Kaiserslautern, 67663 Kaiserslautern, Germany

R. L. Stamps

School of Physics, M013, University of Western Australia, 35 Stirling Highway, Crawley, Western Australia 6009, Australia

(Received 28 October 2007; revised manuscript received 8 January 2008; published 6 March 2008)

We investigate the formation of magnetic domains in a magnetic trilayer patterned using ion beam bombardment. The system consists of a finite array of in-plane magnetized ferromagnetic Fe elements embedded into an antiferromagnetically coupled Fe/Cr/Fe trilayer. Varying the interelement distance, we observe by means of magnetic force microscopy an intriguing transition from individual to collective behavior of the array elements. Above a critical interelement spacing, strong interelement coupling effects are observed, leading to complex correlations between domain structure on individual elements. The mechanism driving these correlations is the formation of domain boundary walls between elements, contrary to the more commonly observed dipolar coupling effects in magnetic arrays fabricated using lithography. Below this critical spacing, the entire array behaves as a single magnetic entity, exhibiting a collective magnetic domain state. The experimental observations can be simulated numerically and explained using an analytical model. The model correctly predicts observed dependencies on interelement distances.

DOI: [10.1103/PhysRevB.77.094405](https://doi.org/10.1103/PhysRevB.77.094405)

PACS number(s): 75.60.Ch, 75.70.Cn, 75.75.+a

I. INTRODUCTION

Pattern formation in the context of magnetic domains offers fascinating studies of complex phenomena in systems that can be studied experimentally with relative ease. The essential features of magnetic domains were first discussed by Landau and Lifshitz,¹ and have been studied since in great detail by numerous authors (see Ref. 2 for an excellent review).

We report here on the formation of magnetic domains in a magnetically inhomogeneous thin film structure. This system consists of a finite array of in-plane magnetized ferromagnetic Fe elements which are embedded into a surrounding, antiferromagnetically coupled Fe/Cr/Fe trilayer. An extensive study of single, isolated elements of this type has been performed in a previous work,³ and this paper is an extension of this work to the case of interacting elements. We find that domain pattern formation in embedded elements displays intriguing and unique collective effects. Most significantly, we show that relevant length scales determining the correlations observed between domains can be controlled completely through ion irradiation and trilayer construction.

The study of small magnetic elements in array geometries attracts considerable attention due to their potential for application as innovative magnetic data storage and programmable logic devices.⁴⁻¹² Usually, these arrays are formed from periodically arranged ferromagnetic “dots” or “islands” which are topographically separated from each other. In these structures, there is no magnetic material between individual elements,¹³ and collective magnetic behavior is determined by long-range dipolar coupling effects (however, see

also Ref. 14). Such dipolar coupling effects have been studied experimentally in a number of contexts⁴⁻¹⁰ and modeled theoretically using micromagnetic simulations.^{11,12}

In the systems studied here, the exchange interaction plays a determining role in mediating effective interactions between array elements. The reason is that the dominant energy determining domain boundaries in our embedded element system is the energy required to form domain walls in the magnetic regions between the elements. These walls set the relevant characteristic length scale for interelement interactions, and can compete with magnetostatic energies in the formation of stable domain patterns. At a critical interelement clearance, determined by these length scales, we observe a transition from an individual to a collective magnetic behavior with regards to the formation of magnetic domains. A simple analytic model is proposed which captures the essential features of the competition between energies. Results are also in qualitative agreement with micromagnetic simulations.

II. EXPERIMENTAL METHODS

The embedded magnetic element array studied in this work was fabricated by local irradiation of an epitaxial, antiferromagnetically coupled Fe/Cr/Fe trilayer with 30 keV Ga⁺ ions. These ions penetrate the multilayer stack and cause structural damage, in particular, within the Cr interlayer region. For sufficiently high fluences, this leads to a local destruction of the interlayer and, thus, to a direct magnetic contact between the two Fe layers. In this way, a local tran-

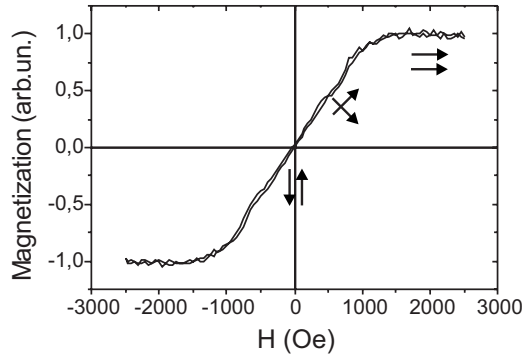


FIG. 1. Magnetization curve recorded from the Fe/Cr/Fe trilayer system studied here before irradiation. The orientations of the two magnetizations are represented by two small black arrows at different values of an externally applied field. A fit to this curve based on the model $E_{\text{IEC}} = -J_1 \cos(\alpha) - J_2 \cos^2(\alpha)$ for the interlayer exchange coupling energy E_{IEC} , where α is the angle between the two magnetizations, yields values of $J_1 = -1 \text{ mJ/m}^2$ and $J_2 = -0.16 \text{ mJ/m}^2$ for bilinear and biquadratic coupling constants, respectively.

sition from antiferromagnetic to ferromagnetic coupling is achieved.^{18,19} It has been shown previously that micron-sized areas which have been irradiated in this way exhibit the properties of small ferromagnetic elements.²⁰ For the experiments discussed in the following, $2 \times 2 \mu\text{m}^2$ square elements of this type were fabricated and were arranged in arrays of 4×4 , with different interelement spacings ranging from 200 nm to $2 \mu\text{m}$.

All arrays are located on the same sample, which was prepared onto a MgO (100) substrate covered by a 1 nm thick Fe seed layer and a 125 nm thick Ag buffer layer by means of electron beam evaporation. The trilayer itself was of the form Fe(10 nm)/Cr(0.7 nm)/Fe(10 nm) and was covered by a 2 nm thick Cr cap layer to prevent oxidation. The exact growth procedure is described elsewhere in more detail.²⁰ Magnetometric measurements by means of the longitudinal magneto-optical Kerr effect confirmed that the sample exhibited a strong antiferromagnetic interlayer exchange coupling in the as-prepared state (see Fig. 1 for a typical magnetization curve). An ALTURA 865 dual beam focused ion beam source was used for the irradiation. In all cases, an ion fluence of $2.7 \times 10^{16} \text{ ions/cm}^2$ was applied. Subsequently, the irradiated structures were investigated by means of magnetic force microscopy (MFM) using a SOLVER NT-MDT magnetic force microscope. This machine was equipped with CoCr coated MFM tips manufactured by VEECO, and was employed in the tapping mode. A distance of 50 nm between tip and sample was chosen to minimize perturbative interactions of the tip stray field with the sample magnetization. Moreover, prior to MFM investigations, the sample was demagnetized by applying an ac field perpendicular to the film plane.

III. EXPERIMENTAL RESULTS

We begin our discussion of MFM images of the array with the largest interelement spacing. Figure 2 contains

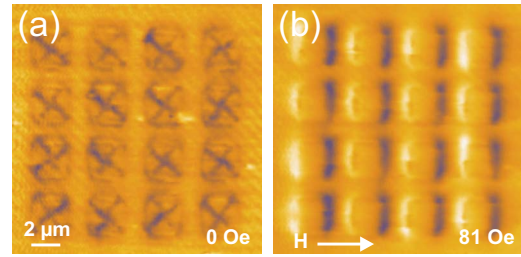


FIG. 2. (Color online) MFM images of an array of $2 \times 2 \mu\text{m}^2$ embedded Fe elements spaced at an interelement distance of $2 \mu\text{m}$ in (a) remanence and (b) saturation at a field of 81 Oe. The direction of the applied magnetic field is indicated by a white arrow in (b).

MFM images of this array with $2 \times 2 \mu\text{m}^2$ elements and an interelement spacing of $2 \mu\text{m}$. Regular patterns of domain walls are clearly visible and define identical domain patterns in each individual element in remanence [Fig. 2(a)] and in saturation [Fig. 2(b)]. There is no indication of interelement interaction since the resulting domain patterns are exactly what one expects for independent square ferromagnetic elements. In this regard, it is also clear that the irradiated regions behave as ferromagnetic particles with strong shape anisotropies created by magnetostatic fields. The regions between ferromagnetic elements do not appear strongly affected by stray dipolar fields, consistent with their antiferromagnetic coupling. During magnetization reversal, no identifiable effects of interelement coupling or other types of collective behavior were observed outside the individual elements.

The situation changes if the spacing between the elements is reduced to $1 \mu\text{m}$ and below. In Fig. 3(a), an atomic force microscope (AFM) image of such an element array is shown, while in Fig. 3(d), the corresponding MFM image in remanence is displayed. It is particularly evident in Fig. 3(d) that the remanent magnetic domain state of an element depends on its position within the array. For example, elements at the array “corners” exhibit a more or less undisturbed Landau domain configuration similar to the remanent configuration of the elements shown in Fig. 3(a). The eight array edge elements, which are not corners, exhibit distorted, asymmetrical Landau-type configurations. The four central elements within the array show remanent magnetic configurations with very little or no resemblance to a Landau pattern. By way of analogy to the distinction between surface and bulk effects in continuous films, these images suggest that there are different perimeter and center environments for elements in the embedded finite array.

We now seek to understand the above observations in terms of effective interelement coupling. In particular, the Landau patterns of central elements appear to be most strongly affected by this coupling due to having four nearest neighbors, whereas elements at the array edges have at most only three near neighbors. Landau patterns of elements at the array corners are affected the least, since they only have two nearest neighbors.

In this interpretation, it is interesting to note that the application of a small external field [as indicated by the white

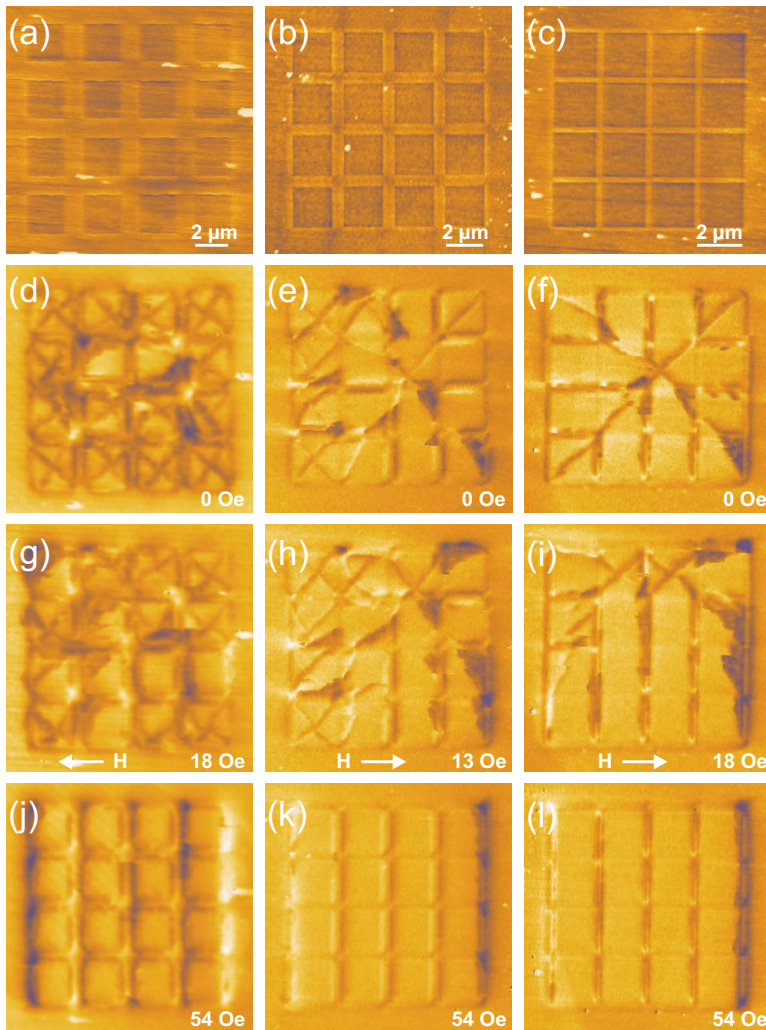


FIG. 3. (Color online) [(a)–(c)] AFM images of arrays of $2 \times 2 \mu\text{m}^2$ embedded Fe elements spaced at distances of (a) $1 \mu\text{m}$, (b) 500 nm , and (c) 200 nm . [(d)–(f)] Corresponding MFM images [(d)–(f)] in remanence, [(g)–(i)] at small field values of 13 or 18 Oe as indicated in the panels, and [(j)–(l)] in saturation at a larger field value of 54 Oe. Each column corresponds to one array. In each case, the direction of the applied magnetic field is indicated by a white arrow in (g), (h), and (i).

arrow in Fig. 3(g)], leaves the magnetic configuration of the corner elements relatively unaffected as compared to that of the remaining elements. This is consistent with our interpretation if we realize that a stable Landau pattern inside a given element requires a particular arrangement of domain walls around the element perimeter in addition to domain walls within the element. Landau patterns in elements with few interelement interactions can, therefore, be more stable than Landau patterns in elements with strong interelement interactions.

This idea has been tested by numerical simulations using a micromagnetic approach. The numerical results are in qualitative agreement with observations, and support our interpretation of the interelement coupling mechanism in terms of domain walls. A discussion of the method and results are given in the Appendix. In Sec. IV, we present a useful model which makes this explicit by taking into account the cost in energy for forming domain walls in the regions between elements and in the regions outside the array.

A saturated single-domain state in all elements is achieved with an applied field value of 54 Oe [Fig. 3(j)], which is significantly smaller than the saturation field value of 81 Oe for the elements shown in Fig. 3(b). These results are consistent with our earlier finding that the saturation field de-

creases if the size of the elements is increased for square elements of $2 \mu\text{m}$ and larger.²¹ This raises a particularly interesting possibility. If an interelement coupling exists within an array of elements, and if the coupling is such that the elements behave as a collective entity, then the array as a whole should behave as a single large element with a reduced saturation field. Hence, also the lateral dimensions of the array should play a role in the magnetization reversal behavior of the elements, in a manner that can be controlled through modifications to the interelement coupling by changing the interelement spacing.

As will be discussed below, this is exactly what is observed in the experiment. For what follows, it is useful to note that according to the above arguments, Landau patterns in the array corner elements should be affected least way by interelement coupling and spacing variations.

A reduction of the interelement spacing to 500 nm clearly demonstrates that a collective magnetic behavior exists. This is illustrated in Fig. 3(b) for an array of elements spaced at 500 nm, and in Fig. 3(e), the corresponding MFM image is displayed in remanence. The array now behaves very much as a single magnetic entity that exhibits a single, large Landau domain structure in remanence. Only some elements at the boundary of this array still exhibit individual magnetic

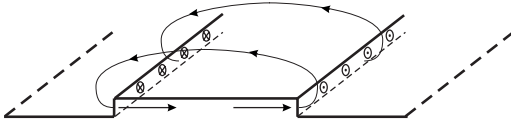


FIG. 4. Schematic illustration of the formation of magnetic surface charges and the associated stray field at topographic step edges of an embedded ferromagnetic element. In this figure, the element is magnetized in a saturated state. The step edges shown in this figure appear between irradiated and nonirradiated areas of the array, are 1–2 nm high, and are created as a side effect of the ion bombardment, which is discussed in detail in Ref. 20. This figure has been adapted from Ref. 3.

properties in the form of smaller Landau configurations. Application of an external field of 13 Oe causes the larger Landau domain structure to change by enlarging the energetically favorable domains, while leaving some smaller Landau configurations at corners and edges stable [Fig. 3(h)]. Although not shown, we have observed that a similar magnetization reversal process for the smaller Landau structures takes place at higher external field values between 27 and 40 Oe when the larger Landau structure has already broken up. Again, at a field value of 54 Oe, the array has reached a saturated single-domain state [Fig. 3(k)]. The magnetic contrast that is still visible within the array in this state has a topographic origin and is caused by stray fields at small, irradiation-induced step edges at the element boundaries (see Fig. 4).

At an element separation of 200 nm, the elements do not exhibit individual properties in remanence. Only a single large Landau structure extending over the whole array can be observed [Fig. 3(f)]. However, at an external field of 18 Oe, when this large Landau structure is in the process of breaking up, the topmost two edge elements of the array exhibit small Landau structures as expected for the more stable edge elements [Fig. 3(i)]. Again, at a field of 54 Oe, the whole array is in a uniformly magnetized single-domain state [Fig. 3(l)], with some magnetic contrast of topographic origin showing up also.

The domain-wall-based effective interelement interaction model proposed above suggests that the observed interelement interactions are governed primarily by exchange and not by dipolar interaction. In particular, related studies on arrays of topographically patterned $2 \times 2 \mu\text{m}^2$ square Fe elements of 20 nm thickness and similar interelement distances did not reveal comparable magnetic configurations.⁹ In that type of system, magnetic coupling effects were, indeed, detected, but were rather weak and did not significantly distort the magnetic domain configuration within individual elements even at very close interelement distances. Due to the topographic separation of the elements, only dipolar interactions can be responsible for the coupling effects observed in Ref. 9. However, within the system studied here, due to the presence of magnetic material between individual elements, interelement coupling can, indeed, be mediated via exchange interaction through the formation of domain walls at the perimeters of elements. We next discuss a model for this interelement interaction.

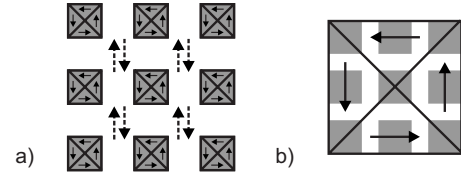


FIG. 5. Micromagnetic configurations assumed in the frame of our analytical model ansatz (a) above and (b) below a critical interelement clearance. Irradiated areas exhibiting ferromagnetic coupling are shaded in gray, while nonirradiated areas exhibiting antiferromagnetic coupling remain white. (a) The magnetization within the embedded ferromagnetic elements is sketched by small solid arrows, while the magnetizations of upper and lower Fe layers in the areas between the elements are given by dashed arrows.

IV. INTERELEMENT INTERACTION AND DISCUSSION

The experimental results displayed in Figs. 1 and 2 lead to the suggestion that there exists a critical interelement spacing w_{crit} , above which the individual array elements behave as separate magnetic entities and below which the array exhibits a collective behavior as a single magnetic system. In the following, we present a model for this critical width.

Let us consider a square array of $N \times N$ embedded ferromagnetic elements, where N is a positive integer. The elements have lateral size L and are spaced (border-to-border) by a distance w [see Fig. 5(a)]. We assume that this distance is large enough such that the individual elements are each magnetized in a Landau configuration, as displayed in Fig. 5(a). In this case, an energy of

$$E^{DW} = 2N^2(2\sqrt{2}Lt\gamma_w^{110} + 4Lt\gamma_w) \quad (1)$$

is needed to form the domain walls appearing in this configuration, where t denotes the thickness of each Fe layer (10 nm in our experiment), and γ_w^{110} and γ_w correspond to the specific domain wall energies of the walls inside and at the boundaries of the elements, respectively.

It has been shown previously that the domain walls at the boundaries of embedded ferromagnetic elements exhibit a complex fine structure, which is, in the case of square elements, not the same for all edges of the square.³ For our purposes, this internal structure is not important, and we make the simplifying assumption that the corresponding domain wall energy can be described by a parameter γ_w with a value roughly equal to that of a 180° (100)-Bloch wall in a material with cubic anisotropy. This energy has been shown to be equal to

$$\gamma_w = 2\sqrt{AK_{c1}}, \quad (2)$$

where A and K_{c1} denote the exchange constant and the first-order cubic anisotropy constant of the respective material.²

The total film thickness is 20 nm inside the embedded Fe elements. For this thickness, we suppose that 90° domain walls in these regions are of a Néel type (see Ref. 22). We approximate the energy of these domain walls by the energy γ_w^{110} of a 90° (110)-Bloch wall in a material with cubic anisotropy. This energy is, according to Ref. 2, equal to

$$\gamma_w^{110} \approx 1.75\sqrt{AK_{c1}} = \frac{7}{8}\gamma_w. \quad (3)$$

The energy needed to form the magnetic vortex in the very center of each Landau configuration is not relevant for the calculations that follow and is neglected.

In what follows, we term the areas between elements as “lanes.” In the configuration displayed in Fig. 5(a), the magnetic moments of the two separate Fe layers in lanes are oriented antiparallel with respect to each other, due to the antiferromagnetic interlayer exchange coupling within these areas. Such an antiparallel alignment leads to a gain in the interlayer magnetic energy. Within an array of $N \times N$ elements, there is a total number of $2(N-1)^2 + 2(N-1)$ lanes and a total number of $(N-1)^2$ lane intersections. Moreover, previous investigations have shown that the domain walls at the boundaries of embedded ferromagnetic elements are located immediately outside of the elements, within the area of these lanes.³ According to the micromagnetic models developed in Ref. 3, the magnetic moments of the upper and lower Fe layers are aligned antiparallel with respect to each other only in a certain part of these domain walls. In the following, we assume that this part has a width of roughly one-half of the total domain wall width Δ . Hence, we will take into account that the width of the lanes in between the individual elements is effectively reduced to a value of $w - 2(1/2)\Delta = w - \Delta$. According to the above considerations, we thus obtain a gain in energy due to antiparallel orientation in the areas between the elements equal to

$$E^{IEC} = -2\{2(N-1)^2 + 2(N-1)\}Lj(w - \Delta) - 2(N-1)^2w^2j, \quad (4)$$

where $j = 1 \text{ mJ/m}^2$ is the absolute value of the bilinear interlayer exchange coupling constant of the system (see, e.g., Ref. 23), which has been derived by means of magneto-optical investigations (see Fig. 1).

Adding up all contributions, one obtains a total energy for the magnetic configuration displayed in Fig. 5(a) of

$$E_{ind} = 2N^2\left(\frac{7}{4}\sqrt{2}Lt\gamma_w + 4Lt\gamma_w\right) - 2\{2(N-1)^2 + 2(N-1)\}Lj(w - \Delta) - 2(N-1)^2w^2j. \quad (5)$$

In a similar manner, a total energy of

$$E_{col} = 2\{[NL + (N-1)w]\sqrt{2}t\frac{7}{4}\gamma_w + [NL + (N-1)w]\}4t\gamma_w + 2\{2(N-1)^2 + 2(N-1)\}Lj(w - \Delta) + 2(N-1)^2w^2j \quad (6)$$

can be approximated for the magnetic configuration displayed in Fig. 5(b).

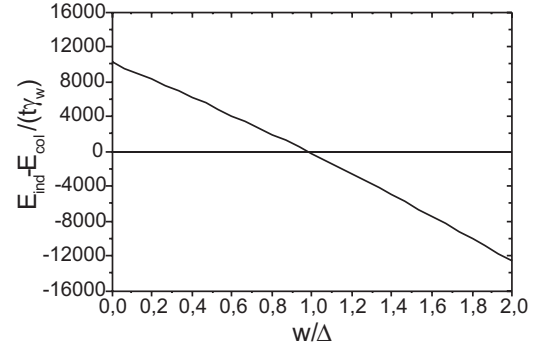


FIG. 6. Function plot corresponding to Eq. (8).

A comparison of these two energies in a dimensionless form yields

$$\begin{aligned} \frac{E_{ind} - E_{col}}{t\Delta\gamma_w} = & \left\{ (N^2 - N)\frac{L}{\Delta} - (N-1)\frac{w}{\Delta} \right\} \frac{7}{2}\sqrt{2} \\ & + 8 \left\{ (N^2 - N)\frac{L}{\Delta} - (N-1)\frac{w}{\Delta} \right\} \\ & - 8\{(N-1)^2 + (N-1)\} \frac{L}{\Delta} \frac{w}{\Delta} \frac{j\Delta}{t\gamma_w} \\ & + 8\{(N-1)^2 + (N-1)\} \frac{L}{\Delta} \frac{j\Delta}{t\gamma_w} - 4(N-1) \frac{w^2}{\Delta^2} \frac{j\Delta}{t\gamma_w}. \end{aligned} \quad (7)$$

In the experimentally investigated system described in Sec. III of this paper, we had the case of $N=4$ and $L=2 \mu\text{m}$. Moreover, previous investigations yielded a domain wall width of $\Delta \approx 500 \text{ nm}$ for this system.³ We, therefore, suppose a value of $L/\Delta \approx 4$ here. Furthermore, using the material parameters $A=2.1 \times 10^{-11} \text{ J/m}$ and $K_{c1}=4.5 \times 10^4 \text{ J/m}^3$ for the exchange constant and first-order anisotropy constant of Fe, respectively,³ we find that $(j\Delta)/(t\gamma_w) \approx 25$.

Substituting these values into Eq. (7) results in a quadratic form in (w/Δ) :

$$\frac{E_{ind} - E_{col}}{t\Delta\gamma_w} = -900\frac{w^2}{\Delta^2} - \left(9624 + \frac{21}{2}\sqrt{2}\right)\frac{w}{\Delta} + 9984 + 168\sqrt{2}. \quad (8)$$

The solution of Eq. (8) for w gives a critical transition width because the energies of the two configurations shown in Fig. 5 should be equal at the transition. A plot of Eq. (8) as a function of (w/Δ) is shown in Fig. 6. One sees that Eq. (8) has a zero at a value of $(w/\Delta) \approx 1$, which corresponds to a critical interelement spacing of $w_{\text{crit}} \approx 500 \text{ nm}$. This value is in good agreement with the MFM based observations discussed in the previous section.

V. CONCLUSION

In conclusion, unique collective magnetic effects were observed by means of magnetic force microscopy in arrays of $2 \times 2 \mu\text{m}^2$ Fe elements embedded into an antiferromagnetically coupled Fe/Cr/Fe trilayer. At a spacing of $1 \mu\text{m}$ between the elements, interelement coupling between ferromagnetic elements was observed, which is primarily mediated by exchange interactions through the formation of domain boundary walls. With decreasing interelement distance, a transition from an individual behavior toward a collective behavior of the array elements is found. At intermediate distances, a superposition of individual and collective domain states can be observed, while at very small distances, the array nearly behaves as a single, homogeneous ferromagnetic entity. The observed phenomena can be understood on the basis of a model where the interelement interactions are determined by energy costs associated with domain wall formation at the perimeter of the elements. Estimates based on this model predict the critical width of the interelement spacing, where a transition between individual and collective behavior is observed.

The findings obtained in the case of an interelement spacing of $1 \mu\text{m}$ are also consistent with the earlier observation that the broad, complex domain walls appearing immediately outside of individual elements have a width of approximately 500 nm .³ Following the above discussion, the lateral range of domain-wall-based magnetic coupling effects between closely spaced embedded elements should be governed by the width of these walls. In particular, it can be expected that elements should interact with each other in this way at interelement distances of twice the wall width, i.e., approximately $1 \mu\text{m}$, and below. This is, indeed, observed in the experiment.

The results obtained in the course of this work clearly show that arrays of embedded ferromagnetic elements exhibit a number of unique magnetostatic properties. Future studies in this field might be devoted to the magnetodynamical properties of these systems, which, due to the important role of exchange interaction, can be expected to differ significantly from those of conventional magnetic element arrays as well.

ACKNOWLEDGMENTS

The authors are indebted to B. Leven for assistance in sample preparation. This work was supported by the European Communities Human Potential Programme HRPN-CT-2002-00296 NEXBIAS and by the Deutsche Forschungsgemeinschaft (HI 380/18). One of the authors (R.L.S.) acknowledges the Australian Research Council for support under a Discovery Project.

APPENDIX

A micromagnetic approach was used to test the idea of a domain wall mediated effective interaction between embedded elements. The model studied was a 2×2 array of magnetic elements. The geometry is defined with the magnetizations in the xy planes of two films, each of thickness d ,

separated by a spacer of thickness t . A magnetic field is applied along the x direction.

The sum of the Zeeman, anisotropy, exchange, and interlayer exchange energies of the two-film system is

$$\frac{E}{Kd} = \sum_{i=1,2} \int \int \left\{ -\lambda_H^2 u_x^{(i)} - \sum_{\alpha \neq \beta} (u_\alpha^{(i)} u_\beta^{(i)})^2 - \lambda_A^2 \sum_{\alpha} u_\alpha^{(i)} (\partial_x^2 u_\alpha^{(i)} + \partial_y^2 u_\alpha^{(i)}) \right\} dx dy + \int \int \frac{\lambda_J(x,y)^2}{d} \sum_{\alpha} u_\alpha^{(1)} u_\alpha^{(2)} dx dy, \quad (\text{A1})$$

where i is 1 for the top film, and 2 for the bottom film. Components of the magnetization are written as $u_\alpha^{(i)} = m_\alpha^{(i)}/M$, where M is the saturation magnetization. Effective lengths contain other magnetic parameters:

$$\lambda_H^2 = \frac{\mu_0 H M}{K} \quad (\text{A2})$$

contains the applied field H , and a fourfold anisotropy K

$$\lambda_A^2 = \frac{A}{K} \quad (\text{A3})$$

contains the ratio of intrafilm exchange A to K , and

$$\lambda_J(x,y)^2 = \frac{J(x,y)}{K} \quad (\text{A4})$$

is the ratio of interlayer exchange J to K . The exchange parameter J is a function of position due to the ion patterning used to define the array. Note that this term is the only one used to define the ferromagnetic and antiferromagnetic regions in the xy plane by defining it positive for elements, and negative for lanes and regions outside the array.

Discretized, this energy is

$$\frac{E}{K\Delta^2 d} = \sum_{n,m} \sum_{i=1,2} \left\{ -\lambda_H^2 u_x^{(i)}(n,m) - \sum_{\alpha \neq \beta} [u_\alpha^{(i)}(n,m) u_\beta^{(i)}(n,m)]^2 - \frac{\lambda_A^2}{\Delta^2} \mathbf{u}^{(i)}(n,m) \cdot \sum_{\delta} [\mathbf{u}^{(i)}(n+\delta, m) + \mathbf{u}^{(i)}(n, m+\delta)] - 4 \frac{\lambda_A^2}{\Delta^2} \right\} + \sum_{n,m} \frac{\lambda_J(n,m)^2}{d} \mathbf{u}^{(1)}(n,m) \cdot \mathbf{u}^{(2)}(n,m), \quad (\text{A5})$$

where the sum over small micromagnetic elements of volume $\Delta^2 d$ within each film is labeled by the integers n and m . The magnetization in each micromagnetic element is assumed to be uniform.

Dipolar energies are also included. The corresponding energy is given in the same notation as a discrete sum over source elements by

$$\frac{E_{dip}}{K\Delta^2 d} = \frac{\lambda_D^2}{2} \sum_{n,m} \sum_{i=1,2} \mathbf{u}^{(i)}(n,m) \cdot [\mathbf{h}^{(i)}(n,m; z=0) + \mathbf{h}^{(i)}(n,m; z=t)], \quad (\text{A6})$$

where

$$\mathbf{h}^{(i)}(n,m;z) = \sum_{n',m'} \left[\frac{\mathbf{u}^{(i)}(n'm')}{r_{\mathbf{k}}^3(z)} - 3 \frac{\mathbf{r}_{\mathbf{k}}(z) \cdot \mathbf{u}^{(i)}(n'm')}{r_{\mathbf{k}}^5(z)} \mathbf{r}_{\mathbf{k}}(z) \right] \quad (\text{A7})$$

with

$$\mathbf{r}_{\mathbf{k}}(z) = \mathbf{x}(n - n') + \mathbf{y}(m - m') + \mathbf{z}(z/\Delta), \quad (\text{A8})$$

$$\mathbf{k} = (n - n', m - m'),$$

and a length

$$\lambda_D^2 = \left(\frac{\mu_o M^2}{K} \right) \left(\frac{d}{\Delta} \right). \quad (\text{A9})$$

Magnetic configurations were calculated iteratively in the following way. First, a starting configuration with magnetization elements parallel within a film but antiparallel between films was chosen. A micromagnetic element $\mathbf{u}(n,m)$ is then chosen and aligned parallel with field defined by $\mathbf{h}(nm) = -\partial_{\mathbf{u}(nm)}(E/Kd\Delta^2)$. This process is repeated for all micromagnetic elements and iterated until a stationary, stable, configuration is found. We note that cutoffs in the dipole sums were used to increase speed. The sums were truncated in the calculation of the dipole field term for each element to a radius of 20 micromagnetic elements.

Parameters used for the simulations were $\lambda_A^2 = 400 \text{ nm}^2$, $\lambda_J^2 = \pm 20 \text{ nm}^2$, $\lambda_D^2 = 0.1$, and $\Delta = 20 \text{ nm}$. The magnetic elements are each $15 \Delta \times 15 \Delta$ in size. Example results are shown in Fig. 7. In Fig. 7(a), the magnetic configuration in the xy plane is shown for the top film with a magnetic element spacing equal to half the element width. With this spacing, the individual elements each display Landau configurations. In Fig. 7(b), the spacing is reduced to 2Δ . The individual Landau configurations are distorted. In Fig. 7(c), the spacing is reduced further to Δ , and the interlayer coupling J set to zero at the perimeter of each magnetic element. Under these conditions, the array behaves as a single square patch with a single, somewhat asymmetrical, Landau con-

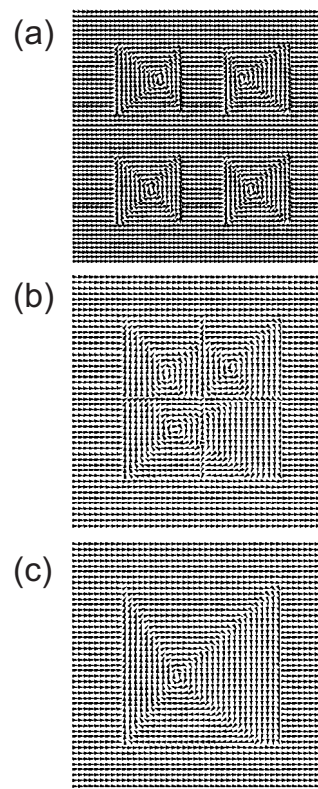


FIG. 7. Magnetic configurations of top film in a 2×2 array of embedded elements. The side of each element is 15Δ . In (a), the spacing between elements is 7Δ . In (b), the spacing is 2Δ , and in (c), the spacing is Δ . The interlayer exchange has been reduced to zero at the perimeter.

figuration. In this model, we were limited by the size of the system that could be practically simulated. Thus, we could not treat sufficiently finely discretized films to describe the domain walls forming in lanes in Figs. 7(b) and 7(c). The need to reduce J at the perimeter for collective behavior may not be necessary in a more finely discretized model.

*Author to whom correspondence should be addressed; sblomeier@t-online.de

¹L. Landau and E. Lifshitz, Phys. Z. Sowjetunion **8**, 153 (1935).
²A. Hubert and R. Schäfer, *Magnetic Domains: The Analysis of Magnetic Microstructures* (Springer, Berlin, 2000).
³S. Blomeier, P. Candeloro, B. Hillebrands, B. Reuscher, A. Brodyanski, and M. Kopnarski, Phys. Rev. B **74**, 184405 (2006).
⁴T. Aign, P. Meyer, S. Lemerle, J. P. Jamet, J. Ferré, V. Mathet, C. Chappert, J. Gierak, C. Vieu, F. Rousseaux, H. Launois, and H. Bernas, Phys. Rev. Lett. **81**, 5656 (1998).
⁵C. Mathieu, C. Hartmann, M. Bauer, O. Buettner, S. Riedling, B. Roos, S. O. Demokritov, B. Hillebrands, B. Bartenlian, C. Chappert, D. Decanini, F. Rousseaux, E. Cambril, A. Müller, B. Hoffmann, and U. Hartmann, Appl. Phys. Lett. **70**, 2912 (1997).
⁶Y. B. Xu, A. Hirohata, L. Lopez-Diaz, H. T. Leung, M. Tselepi, S. M. Gardiner, W. Y. Lee, J. A. C. Bland, F. Rousseaux, E. Cam-

bril, and H. Launois, J. Appl. Phys. **87**, 7019 (2000).

⁷J. Jorzick, C. Krämer, S. O. Demokritov, B. Hillebrands, E. Sondergard, M. Bailleul, C. Fermon, U. Memmert, A. N. Müller, A. Kouna, U. Hartmann, and E. Tsybal, J. Magn. Magn. Mater. **226-230**, 1835 (2001).
⁸R. Hyndman, A. Mougín, L. C. Sampaio, J. Ferré, J. P. Jamet, P. Meyer, V. Mathet, C. Chappert, D. Mailly, and J. Gierak, J. Magn. Magn. Mater. **240**, 34 (2002).
⁹M. Bolte, R. Eiselt, G. Meier, D.-H. Kim, and P. Fischer, J. Appl. Phys. **99**, 08H301 (2006).
¹⁰V. Repain, J.-P. Jamet, N. Vernier, M. Bauer, J. Ferré, C. Chappert, J. Gierak, and D. Mailly, J. Appl. Phys. **95**, 2614 (2004).
¹¹R. L. Stamps and R. E. Camley, Phys. Rev. B **60**, 11694 (1999).
¹²L. F. Zhang, C. Xu, P. M. Hui, and Y. Q. Ma, J. Appl. Phys. **97**, 103912 (2005).

- ¹³There is also a special case known to the authors where arrays of Fe (110) nanowires on stepped W (110) surfaces were studied experimentally (Refs. 15 and 16). These systems consisted of very thin magnetic elements [between 1.4 and 1.8 ML (monolayer) thick] that were surrounded by a 1 ML thick pseudomorphic Fe layer. Magnetic coupling effects, leading to antiferromagnetic order, were also observed in this system and were, also in this case, identified to be of dipolar origin. A growth-induced rotation of the magnetic easy axis into out-of-plane orientation within the elements was identified as the origin of the observed effects (Ref. 17). Hence, within these systems, the 1 ML Fe layer in between the elements did not play a principal role in mediating the observed interelement coupling.
- ¹⁴The results obtained by Repain *et al.* (Ref. 10) are a notable exception to the usual findings that magnetic coupling effects in lithographically patterned element arrays are of purely dipolar nature. In their work, the authors study magnetic interactions in Pt/Co/Pt dot arrays with perpendicular anisotropy and single-domain configurations. These arrays were fabricated by means of focused ion beam milling. Varying the applied ion fluence in the areas between the array elements, the authors were able to realize different degrees of separation between the elements. Magneto-optical investigations of this system yielded a transition from a dipolar to an exchange dominated coupling behavior of the dots with decreasing degree of separation.
- ¹⁵J. Hauschild, U. Gradmann, and H. J. Elmers, *Appl. Phys. Lett.* **72**, 3211 (1998).
- ¹⁶O. Pietzsch, A. Kubetzka, M. Bode, and R. Wiesendanger, *Phys. Rev. Lett.* **84**, 5212 (2000).
- ¹⁷N. Weber, K. Wagner, H. J. Elmers, J. Hauschild, and U. Gradmann, *Phys. Rev. B* **55**, 14121 (1997).
- ¹⁸S. O. Demokritov, C. Bayer, S. Poppe, M. Rickart, J. Fassbender, B. Hillebrands, D. I. Kholin, N. M. Kreines, and O. M. Liedke, *Phys. Rev. Lett.* **90**, 097201 (2003).
- ¹⁹V. E. Demidov, D. I. Kholin, S. O. Demokritov, B. Hillebrands, F. Wegelin, and J. Marien, *Appl. Phys. Lett.* **84**, 2853 (2004).
- ²⁰S. Blomeier, B. Hillebrands, V. E. Demidov, S. O. Demokritov, B. Reuscher, A. Brodyanski, and M. Kopnarski, *J. Appl. Phys.* **98**, 093503 (2005).
- ²¹S. Blomeier, P. Candeloro, B. Hillebrands, B. Reuscher, A. Brodyanski, and M. Kopnarski, *J. Magn. Magn. Mater.* **310**, 2353 (2007).
- ²²M. Schneider, S. Müller-Pfeiffer, and W. Zinn, *J. Appl. Phys.* **79**, 8578 (1996).
- ²³D. E. Bürgler, P. Grünberg, S. O. Demokritov, and M. T. Johnson, in *Handbook of Magnetic Materials*, edited by K. J. H. Buschow (Elsevier, Amsterdam, 2001), Vol. 13.